Midazolam Exhibits Characteristics of a Highly Permeable P-Glycoprotein Substrate

Sanna Tolle-Sander,[1] Jarkko Rautio,[2] Steve Wring,[3] Joseph W. Polli,[4] and James E. Polli[1,5]

Received January 3, 2002; accepted January 13, 2003

Purpose. The purpose of this study was to investigate whether midazolam exhibits characteristics of a highly permeable P-glycoprotein (P-gp) substrate and to evaluate the potential influence of P-gp inhibition on 1-OH midazolam formation during midazolam transport.
Methods. P-gp interaction was investigated by P-gp ATPase assay, efflux inhibition studies, and transport studies of midazolam across MDR1-MDCK and 1-α,25-dihydroxy vitamin D_3-induced Caco-2 monolayers with and without the P-gp inhibitor GF120918.
Results. Midazolam was highly permeable and transport appeared essentially unpolarized. In MDR1-MDCK, the basolateral-to-apical (B-to-A) permeability was slightly higher (16%) than apical-to-basolateral (A-to-B) permeability ($p = 0.04$); GF120918 increased A-to-B permeability by 27% ($p = 0.01$), and increased cellular midazolam accumulation during A-to-B transport by 45% ($p = 0.01$). Midazolam (200 μM) decreased rhodamine123 and vinblastine B/A ratios 3-fold ($p < 0.006$), while increasing their cellular accumulation ($p < 0.003$). P-gp ATPase activation by midazolam was dose-dependent and saturable [$K_m = 11.5(\pm 4.0)$ μM; $V_{max} = 41.1(\pm 7.4)$ nmol/mg/min]. P-gp inhibition increased 1-OH midazolam formation in A-to-B studies 1.3-fold when midazolam donor ≥10 μM ($p < 0.03$). In B-to-A studies, P-gp inhibition did not significantly increase metabolite formation ($p = 0.06$). Midazolam's extraction ratio was not influenced by P-gp ($p = 0.2$).
Conclusions. The results indicate that midazolam exhibited characteristics of a highly permeable P-gp substrate. 1-OH midazolam formation during A-to-B midazolam transport increased slightly when P-gp was inhibited.

KEY WORDS: midazolam; P-glycoprotein; high permeability; metabolism; 1-hydroxy midazolam.

INTRODUCTION

Drug efflux by P-glycoprotein (P-gp) and intestinal drug metabolism by cytochrome P450 (CYP) 3A can each reduce oral bioavailability and cause drug-drug interactions (1–5). Additionally, many compounds are dual substrates for P-gp and CYP3A (6,7). Recent evidence suggests a synergistic effect of these proteins in reducing the intestinal absorption of dual P-gp/CYP3A substrates. P-gp is proposed to increase drug metabolism by increasing the exposure of drugs to CYP3A, caused by repeated efflux and reabsorption into epithelial cells during the passage along the intestinal tract (5,7–10).

In the assessment of potential P-gp substrates, the issue of passive drug permeability merits consideration because high passive permeability may mask measurable P-gp efflux. Polarized transport is preferentially exhibited by P-gp substrates with moderate passive membrane permeability (11–13). For such compounds, P-gp efflux from the cell competes against passive drug influx, resulting in appreciable polarized transport. In contrast, high permeability substrates exhibit rapid trans-membrane movement (9,12,14), which allows permeation into the cell to be significantly faster than P-gp efflux. As a result, transport of these substrates is practically not polarized despite drug efflux. Additionally, low permeability substrates may not achieve an intracellular or bilayer concentration that would result in notable P-gp efflux, yielding unpolarized transport. Thus, it may be difficult to identify P-gp substrates that exhibit permeability outside the moderate range.

The general aim of this study was to probe the interplay of P-gp and CYP3A, under the limiting condition of a drug possessing high passive membrane permeability. Midazolam was selected because it exhibits high passive permeability *in vivo*, with a site of action within the central nervous system (15,16), and because it is a CYP3A substrate. Midazolam oral bioavailability is low (36%) because of first pass metabolism, of which 43% occurs in intestinal cells during absorption (1). Consistent with its anticipated high passive permeability, midazolam has not generally been identified as a P-gp substrate, although it has been characterized as a nontransported substrate (13).

Given midazolam's susceptibility for intestinal CYP3A metabolism and a propensity for CYP3A substrates to be P-gp substrates, we hypothesized that midazolam is a P-gp substrate. Further, given a possible interplay between P-gp and CYP3A to reduce drug absorption, we proposed that midazolam's metabolism to 1-OH MDZ would be modulated by P-gp.

The objectives of this study were to assess whether midazolam exhibits characteristics of a highly permeable P-gp substrate and to evaluate the influence of P-gp inhibition on 1-OH MDZ formation during midazolam transport. As the results show, midazolam appears to be a high permeability P-gp substrate. P-gp inhibition resulted in a slight increase in 1-OH MDZ formation. Interestingly, based upon an *in vivo* model for the interplay of P-gp and CYP3A functioning (7,10), our initial expectation was that P-gp inhibition of midazolam would result in less 1-OH MDZ formation. However, *in vitro* results across cell monolayers showed the opposite effect.

MATERIALS AND METHODS

Materials

MDR1-MDCK cells were donated by Dr. Michael Gottesman (NIH; Bethesda, MD, USA). Midazolam was supplied from Ultrafine (Manchester, UK); the P-gp inhibitor GF120918 from GlaxoSmithKline (Research Triangle Park, NC, USA); Caco-2 cells from ATCC (Manassas, VA, USA);

[1] Department of Pharmaceutical Sciences, University of Maryland, 20 N Pine Street, Baltimore, Maryland.
[2] Department of Pharmaceutical Chemistry, University of Kuopio, Kuopio, Finland.
[3] Preclinical Drug Metabolism and Pharmacokinetics, Trimeris, Durham, North Carolina.
[4] Preclinical Drug Metabolism and Pharmacokinetics, GlaxoSmithKline, Research Triangle Park, North Carolina.
[5] To whom correspondence should be addressed. (jpolli@rx.umaryland.edu)

0724-8741/03/0500-0757/0 © 2003 Plenum Publishing Corporation

Dulbecco's modified Eagle's medium (DMEM), Hank's balanced salt solution, phosphate-buffered saline, rhodamine 123, sodium selenite, zinc sulfate, DL-alpha-tocopherol, 1-α,25-dihydroxy vitamin D_3, and laminin were from Sigma Chemical Co. (St. Louis, MO, USA); HEPES buffer (1 M, pH7.0) and NEAA were from Biofluids (Rockville, MD, USA); fetal bovine serum (FBS) and antibiotic-antimycotic solution were from Life Technologies, Inc. (Rockville, MD, USA); Transwells® with polycarbonate filters (0.45 μm) was from Corning Costar Corporation (Cambridge, MA, USA); Biocoat PET inserts (3.0 μm) were from Beckton Dickinson (Bedford, MA, USA); radiolabeled ^{14}C-mannitol (51.5 mCi/mmol) was from Moravek Pharmaceuticals (Brea, CA, USA); ^{3}H-vinblastine sulphate (12.5 Ci/mmol) was from Amersham Pharmacia Biotech (Little Chalfont, UK); Econosafe was from RPI (Mount Prospect, IL, USA); and human P-gp ATPase assay membranes from Gentest (Woburn, MA, USA). All other ATPase assay components were obtained from Sigma Chemical Co. Water was purified. Organic solvents were high-performance liquid chromatography grade.

Cell Culture

All cells were grown at 37°C, 90% relative humidity, and 5% CO_2 atmosphere, and fed every 2–3 days. MDR1-MDCK cells were grown in DMEM with 10% FBS and 80 ng/mL colchicine up to 90% confluence before plating at 600,000 cells/cm^2 onto Transwells® (0.45 μm, 4.71 cm^2) for 6 days. Caco-2 cells at passage 41–43 were grown in Dulbecco's modified Eagle's medium (supplemented with 10% FBS, 1% NEAA, 50 U/mL penicillin, 50 μg/mL streptomycin, and 0.125 μg/ml amphotericin B) to 90% confluency before seeding onto laminin-handcoated (5 μg/cm^2) Biocoat® PET Inserts (3 μm, 4.2 cm^2) at 63,000 cells/cm^2. After day 7, the cells were grown in the above medium containing only 5% FBS until day 21. Induced cells were additionally supplemented with 0.1 μM sodium selenite, 3 μM zinc-sulfate, 45 nM DL-α-tocopherol, and 0.25 μM 1-α,25-dihydroxy vitamin D_3 (17).

Transport Studies

Transport studies were conducted at 37°C, pH 6.8, and 50 rpm, after three Hank's balanced salt solution washes of each monolayer. Midazolam (5 μM) flux across MDR1-MDCK monolayers was performed in apical-to-basolateral (A-to-B) and basolateral-to-apical (B-to-A) directions with and without 500 nM GF120918. Rhodamine 123 (10 μM) and vinblastine (20 nM) flux was measured in the absence and presence of 500 nM GF120918, 200 μM midazolam, or 40 μM 1-OH MDZ.

Across uninduced Caco-2 monolayers, A-to-B flux was measured at 5, 25, and 100 μM midazolam and B-to-A flux at 5 μM. In induced Caco-2 cells, midazolam flux was measured at donor concentrations 5, 10, 25, and 100 μM A-to-B and 5 and 10 μM B-to-A. Additionally, the effect of the P-gp inhibitor GF120918 (500 nM) was investigated. GF120918 has a negligible effect on CYP3A4 (18). 1-OH MDZ and 4-OH MDZ transport was measured at 10 μM in both directions. Receivers were sampled after 40, 80 and 120 min, and donors after 120 min. Samples were assayed for midazolam, 1-OH MDZ, and 4-OH MDZ. The major human metabolite 1-OH MDZ appeared in all midazolam samples, and its formation was linear with time (data not shown). 4-OH MDZ was below the limit of quantification (i.e. 0.5 nM).

Mass balance ranged between 85–105%. Mannitol was used to assess monolayer integrity. For un-induced and induced Caco-2 cells, rhodamine 123 (10 μM) A-to-B and B-to-A permeability was used to assess P-gp expression. No difference was detected in either P-gp expression or mannitol permeability between un-induced and induced cells ($p > 0.3$).

The extraction ratio (ER) was calculated according to Eq. (1), which was adopted from Fisher *et al.* (19):

$$\mathrm{ER} = \frac{metabolite_{(\mathrm{donor,receiver})}}{midazolam_{(\mathrm{receiver})} + metabolite_{(\mathrm{donor,receiver})}} \quad (1)$$

where ER is the extraction ratio, $metabolite_{(\mathrm{donor,\ receiver})}$ is the sum of 1-OH MDZ quantities in the donor and receiver, and $midazolam_{(\mathrm{receiver})}$ is the quantity of midazolam in the receiver.

Human P-gp ATPase Assay

In P-gp containing membranes, inorganic phosphate released by P-gp ATPase in the presence of drug was quantified; P-gp specific ATPase activity was indicated by the difference in phosphate produced with and without orthovanadate (20). In a plate reader format, midazolam (2.5, 5, 10, 25, and 100 μM), 1-OH MDZ, and 4-OH MDZ (10 and 100 μM) were incubated for 20 min with P-gp membranes in at least duplicate wells and quantified by a colorimetric assay. The activation ratio refers to change in P-gp specific phosphate release by membranes incubated with and without drug. Verapamil (20 μM) and rhodamine (10 μM) served as positive control. A simple $E_{\max}$ model was used to model effect of midazolam concentration on ATPase activity (WinNonlin 1.0, Pharsight, Mountain View, CA, USA).

Analysis

Midazolam was quantified by HPLC-UV using a Waters system equipped with 486 tunable absorbance detector at 220 nm, 510 pump, and 717 plus autosampler. The column was a BDS-Hypersil 150 × 4.6 mm (Keystone Scientific, Bellefonte, PA, USA). Flow rate was 1.0 mL/min and mobile phase contained 47:43:10 of phosphate buffer (20 mM, pH 6.7):acetonitrile:methanol.

Midazolam hydroxy metabolites were analyzed by means of LC/MS/MS on a Hewlett Packard 1100, equipped with a Gilson 215 autosampler and either a PESciex API2000 or API3000 mass spectrometer. The column was a Phenomenex Develosil C18 50 × 2 mm 3μm, heated to 40°C. Flow rate was 0.7 mL/min, and mobile phase contained a gradient of 1–40% acetonitrile in ammonium formate (10 mM formic acid adjusted to pH 3.5 with ammonium hydroxide). Detection by positive ion electrospray tandem mass spectrometry was achieved using the precursor to product ion transitions that afforded the greatest response for each metabolite. Midazolam and its metabolites were resolved chromatographically. The total amount metabolite found in the donor was corrected for small amounts of each compound present before initiation of the study.

^{14}C-Mannitol and ^{3}H-vinblastine were quantified using a Beckman liquid scintillation counter model LS 5801, in Econosafe scintillation cocktail. Rhodamine 123 was quantified

using a platereader (Wallac Victor^2, Perkin–Elmer, Wellesley, MA, USA) set to excitation 495 nm and emission 514 nm. Each sample was measured in at least duplicate wells.

Statistical Analysis

Results were analyzed by Student *t* test or analysis of variance with post hoc analysis using SPSS version 10 (SPSS Inc; Chicago, IL). A p value <0.05 was considered significant. SEM of ratios were calculated by the delta-method (21).

RESULTS

High Midazolam Permeability and Minimal Apparent Polarized Transport

In Table I, midazolam permeability across un-induced and induced Caco-2 monolayers was high, with permeability above 30×10^{-6} cm/s, similar to previous findings (19). Midazolam permeabilities exceeded metoprolol permeabilities, which are typically 25×10^{-6}cm/s, indicating high midazolam permeability (22). High midazolam permeability was expected since midazolam is a rapidly absorbed (16,23) central nervous system agent with high lipophilicity (logP > 3.5; Ref. 24).

In Table I, midazolam transport across induced Caco-2 monolayers generally did not appear to be polarized, with B/A transport ratios close to unity at all midazolam donor concentrations (5–100 μM), regardless of whether GF120918 was present or absent. The B-to-A permeability was significantly higher than A-to-B permeability ($p = 0.002$) only when midazolam donor was 5 μM. The monolayers expressed P-gp, since rhodamine 123 yielded a B/A ratio of 6.01.

Similar results were observed across un-induced Caco-2 monolayers (data not shown). Midazolam permeability was not polarized across un-induced Caco-2 monolayers, even at 5 μM midazolam ($p = 0.4$). The A-to-B and B-to-A permeabilities were not dependent upon concentration (analysis of variance, $p = 0.13$). Functional P-gp expression in uninduced monolayers was demonstrated by a rhodamine 123 B/A ratio of 6.29 (±0.92).

Hence, in Caco-2 monolayers, midazolam B-to-A transport ratio did not practically differ from unity, and GF120918 did not affect midazolam permeability.

Midazolam transport across MDR1-MDCK monolayers was similar to transport across Caco-2 monolayers, although reflected greater midazolam efflux across MDR1-MDCK monolayers than Caco-2 monolayers. Midazolam permeability for 5 μM donor midazolam across MDR1-MDCK cells was high and appeared to be practically unpolarized. In Fig. 1, the B-to-A ratio of midazolam alone was 1.16 (±0.05). The B-to-A permeability of 56.9 (±2.2) $\times 10^{-6}$ cm/s was slightly higher than the A-to-B permeability of 49.1 (±0.7) $\times 10^{-6}$ cm/s ($p = 0.04$). Although midazolam B-to-A permeability at 61.1 (±5.4) was unchanged by GF120918 ($p = 0.26$), A-to-B permeability was increased by GF120918 to 62.4 (±2.2) $\times 10^{-6}$ cm/s ($p = 0.014$), which may perhaps suggest some manifestation of P-gp transport of midazolam. More notable was the enhancement of intracellular midazolam retention when GF120918 was present. In Fig. 2, from A-to-B studies, midazolam amount in cell lysate increased 1.45-fold from 116 (±11) nmol/monolayer to 169 (±2) nmol/monolayer when GF120918 was present ($p = 0.007$). Rhodamine 123 and vinblastine yielded a B/A ratio of 7.17 (±0.79) and 7.63 (±0.57), respectively, indicating P-gp expression.

Transport studies of 1-OH MDZ and 4-OH MDZ across uninduced Caco-2 cells were conducted. Like midazolam, they exhibited high permeability, which did not appear to be polarized, i.e., B-to-A ratio was close to unity (Table I). However, 4-OH MDZ had a slightly higher B-to-A permeability than A-to-B permeability ($p = 0.01$). There was no difference in the directional permeabilities for 1-OH MDZ ($p > 0.29$).

Midazolam Inhibition of Rhodamine 123 and Vinblastine Efflux

The above midazolam permeability data indicates that P-gp did not markedly affect midazolam transport. Neverthe-

Table I. Permeability of Midazolam and Hydroxy-Metabolites across Caco-2 Cells

Compound	Concentration (μM)	A-to-B permeability ($\times 10^6$ cm/s)	B-to-A permeability ($\times 10^6$ cm/s)	Ratio
Midazolam[a,b]	5	37.9 (±0.8)	42.7 (±0.1)	1.13 (±0.02)
	10	39.4 (±1.5)	42.1 (±1.8)	1.07 (±0.06)
	25	34.8 (±0.1)	NA	NA
	100	34.3 (±1.5)	NA	NA
Midazolam plus GF120918[a,c]	5	36.2 (±1.0)	36.9 (±6.5)	1.02 (±0.18)
	10	37.1 (±1.0)	36.5 (±1.2)	0.98 (±0.03)
	25	38.7 (±3.1)	NA	NA
	100	39.2 (±1.9)	NA	NA
1-OH-MDZ[d]	10	40.5 (±0.8)	39.4 (±1.7)	0.97 (±0.05)
4-OH-MDZ[d]	10	27.4 (±0.6)	32.1 (±0.7)	1.17 (±0.04)
Rhodamine 123[a]	10	0.649 (±0.025)	3.90 (±0.03)	6.01 (±0.25)

Note: Values in brackets are SEMs of at least triplicate determinations. NA denotes not performed.
[a] Caco-2 monolayers were CYP3A-induced by 1-α,25-dihydroxy vitamin D_3 containing medium.
[b] Permeability values across un-induced and induced Caco-2 monolayers were not different ($p > 0.3$).
[c] GF120918 concentration was 500 nM.
[d] Cell monolayers were not CYP3A induced.

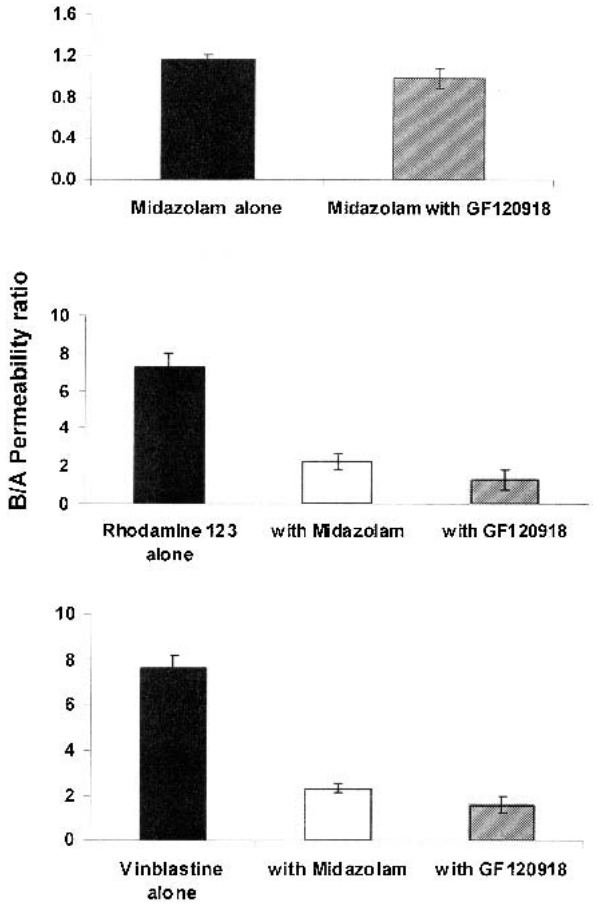

Fig. 1. B-to-A permeability ratio of vinblastine, rhodamine 123 and midazolam in MDR1-MDCK cells. Midazolam concentration was 5 μM in midazolam transport studies and 200 μM in inhibition studies of vinblastine and rhodamine 123. Concentrations of vinblastine, rhodamine 123, and GF120918 were 20 nM, 10 μM, and 500 nM, respectively. Values are given with SEMs of at least triplicate determinations. Drug alone (filled bars), with midazolam (unfilled bars), with GF120918 (hatched bars).

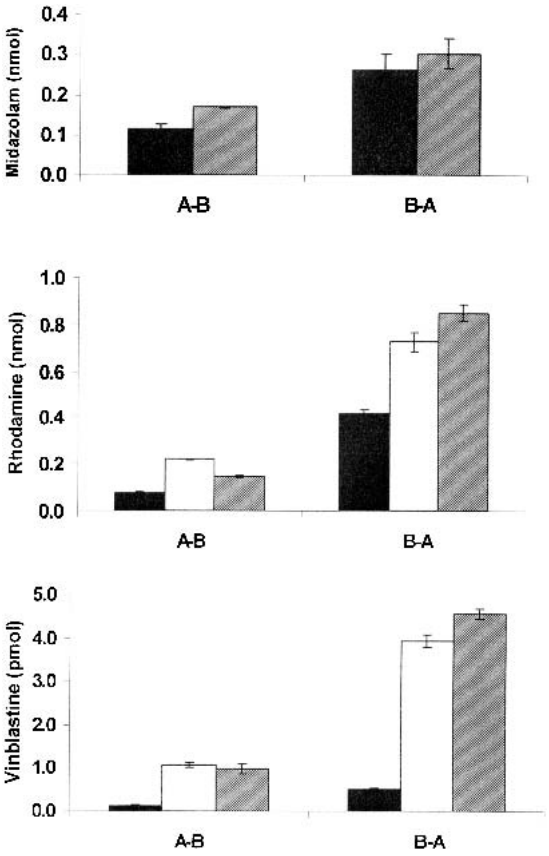

Fig. 2. Cellular uptake of vinblastine, rhodamine 123 and midazolam in MDR1-MDCK cells after transport. Midazolam concentration was 5 μM in midazolam transport studies and 200 μM in inhibition studies of vinblastine and rhodamine 123. Quantities of intracellular midazolam, rhodamine 123, and vinblastine were obtained after 90 min of transport. Values are given with SEMs of at least triplicate determinations. Legend: drug alone (filled bars), with midazolam (unfilled bars), with GF120918 (hatched bars).

less, the high permeability of midazolam allows for the possibility that midazolam is a P-gp substrate, whose transport cannot be practically modulated by P-gp (11). Because of this possibility, the interaction of midazolam with P-gp was investigated via midazolam inhibition of rhodamine 123 and vinblastine, and by activation of P-gp ATPase by midazolam.

Figure 1 illustrates midazolam's inhibition of P-gp efflux of rhodamine 123 and vinblastine across MDR1-MDCK cells. The B/A transport ratio of rhodamine 123 alone was 7.17 (±0.79), whereas the presence of midazolam reduced the ratio to 2.22 (±0.42) ($p = 0.006$). GF120918 reduced the ratio to about 1.0. The A-to-B permeabilities of rhodamine 123 alone, with midazolam, and with GF120918 were 0.374 (±0.037), 0.435 (±0.081), and 0.562 (±0.151) $\times 10^{-6}$ cm/s, respectively. The corresponding B-to-A permeabilities were 2.68 (±0.14), 0.964 (±0.040) and 0.649 (±0.034) $\times 10^{-6}$ cm/s.

Similarly, in Fig. 1, the B-to-A transport ratio for vinblastine alone was 7.63 (±0.57), which was reduced to 2.30 (±0.20) by midazolam ($p = 0.006$). GF120918 reduced the ratio to about 1.5. A-to-B permeabilities of vinblastine alone, with midazolam, and with GF120918 were 0.758 (±0.029), 1.00 (±0.03), and 1.24 (±0.28) $\times 10^{-6}$ cm/s, respectively. The corresponding B-to-A permeabilities were 5.78 (±0.37), 2.29 (±0.19) and 1.97 (±0.07) $\times 10^{-6}$ cm/s.

In Fig. 2, midazolam increased the amount of rhodamine 123 and vinblastine in cell lysates during these inhibition studies. After A-to-B transport, intracellular rhodamine 123 increased from 77.4 (±5.8) pmol/monolayer to 220 (±3) pmol/monolayer ($p = 0.001$); after B-to-A transport rhodamine 123 increased from 419 (±14) pmol/monolayer to 726 (±7) pmol/monolayer ($p = 0.003$). Likewise, midazolam increased cell-associated vinblastine after A-to-B transport nearly 10-fold, from 0.123 (±0.018) pmol/monolayer to 1.06 (±0.06) pmol/monolayer, and more than 8-fold after B-to-A transport, from 0.492 (±0.032) pmol/monolayer to 3.93 (±0.15) pmol/monolayer ($p < 0.0008$ for each). These observations are consistent with midazolam's enhancement of calcein-AM into MDR1-MDCK cells (13). Midazolam's inhibition of the P-gp efflux of vinblastine and rhodamine 123 suggests midazolam to interact with P-gp, at least as an inhibitor.

Midazolam Activation of P-gp ATPase

Human P-gp ATPase containing membranes were used to further investigate whether midazolam activates human P-gp ATPase. Figure 3 shows midazolam to activate P-gp

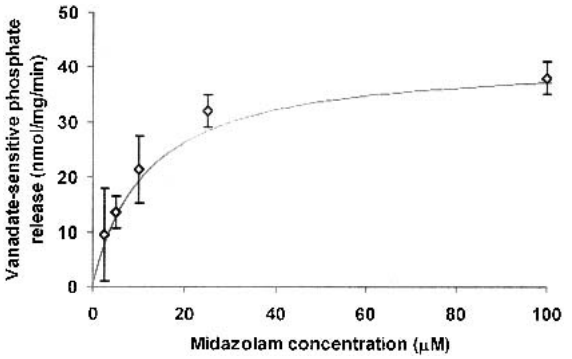

Fig. 3. Concentration-dependent activation of P-gp ATPase by midazolam. ATPase activation by midazolam was concentration-dependent and saturable. From a simple E_{max} model, K_m was 11.5 (±4.0) μM, and V_{max} 41.1 (±7.4) nmol/mg/min. Values in brackets are SEMs from three determinations.

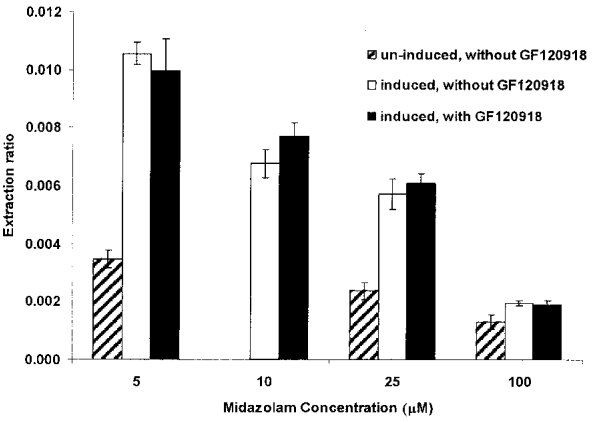

Fig. 4. Extraction ratio of midazolam across Caco-2 cells in the A-to-B direction. Monolayers were either un-induced or induced. GF120918 was either present or absent. Values in brackets are SEMs from three determinations.

ATPase in a concentration-dependent, saturable fashion. The K_m and V_{max} were estimated to be 11.5 (±4.0) μM and 41.1 (±7.4) nmol/mg/min, respectively. Midazolam at 10, 25, and 100 μM concentrations activated ATPase 2, 3, and 3.6-fold over drug-free membranes, respectively, indicating P-gp activation at higher midazolam concentrations. Midazolam activation ratio was significantly different from drug-free control at 25 and 100 μM midazolam ($p < 0.025$). At low midazolam concentrations of 2.5 and 5 μM, no P-gp ATPase activation occurred (activation 0.9 and 1.3-fold, respectively). These results may indicate that midazolam requires a threshold concentration for measurable ATPase activation. The known P-gp substrates verapamil (20 μM) and rhodamine 123 (10 μM) activated P-gp ATPase 5.6 and 3.4-fold, respectively, which suggests that midazolam has a lower affinity for P-gp.

1-OH MDZ and 4-OH MDZ were also evaluated for P-gp ATPase activation. Although 10 μM 1-OH MDZ did not cause activation ($p = 0.05$), 100 μM 1-OH MDZ activated P-gp ATPase 1.7-fold ($p = 0.009$). Meanwhile, 10 and 100 μM 4-OH MDZ activated P-gp ATPase 2.2 and 4.3-fold ($p = 0.004$ and 0.0002), respectively, which are similar to midazolam values.

Increased 1-OH MDZ Formation with P-gp Inhibition

The above results indicate midazolam to exhibit high membrane permeability, which was concentration-independent and apparently not polarized. However, results also show midazolam to stimulate P-gp ATPase and function as an inhibitor of P-gp transport. Because midazolam is metabolized during transport across induced Caco-2 monolayers, the effect of P-gp inhibition on midazolam metabolism was investigated to further evaluate the possibility of midazolam being a high permeability P-gp substrate.

In Fig. 4, the midazolam extraction ratio (ER) across induced Caco-2 monolayers (i.e. across 1-α,25-dihydroxy vitamin D_3 treated monolayers) was generally two to three times larger than across un-induced Caco-2 monolayers ($p < 0.01$, except at 100 μM, $p = 0.09$). Cell treatment with 1-α,25-dihydroxy vitamin D_3 was previously shown to induce midazolam CYP3A metabolism (19). The cumulative amount of 1-OH MDZ found after 120 min was approximately 5-fold less than amounts reported by Fisher *et al.* (19). The Caco-2 cells used in the present study were not selected for high CYP3A expression, which may partly account for this difference (17,19).

In Fig. 5, the cumulative amount of extracellular 1-OH MDZ metabolite after 120 min generally increased with increasing midazolam donor concentration. While the studied midazolam concentration did not exceed 100 μM and no saturation was observed, the metabolism profiles in Fig. 5 are qualitatively consistent with previous observations that midazolam K_m for CYP3A4 was 9.1 μM in Caco-2 cells (19). Un-induced cells resulted in less 1-OH MDZ to be formed. In A-to-B midazolam flux studies across induced cells, the cumulative amounts of formed 1-OH MDZ from 5, 10, 25 and 100 μM midazolam donor concentrations were 47.6 (±1.4), 59.0 (±4.0), 108 (±8), and 154 (±3) pmol/monolayer without GF120918, and 42.4 (±4.7), 74.3 (±4.1), 151 (±4), and 190 (±6) pmol/monolayer with GF120918, respectively. Hence, the ratios of cumulative 1-OH MDZ produced with GF120918 vs. without GF120918 were 0.891 (±0.100), 1.26 (±0.11), 1.40 (±0.11), and 1.23 (±0.05) at 5, 10, 25, and 100 μM midazolam donor, respectively. Interestingly, the amount of 1-OH MDZ found in the extracellular compartments in A-B samples increased when GF120918 was present ($p < 0.03$), except at 5 μM midazolam ($p = 0.2$). These data indicated an approxi-

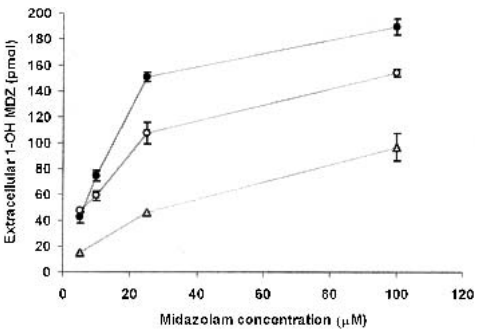

Fig. 5. Generation of 1-OH MDZ into apical and basolateral compartments during midazolam transport across induced Caco-2 monolayers. A-to-B with GF120918 (closed circles), A-to-B without GF120918 (open circles), A-to-B without GF120918 in uninduced cells (open triangles). Values in brackets are SEMs from three determinations.

mate 25% increase in midazolam metabolism at higher midazolam concentration because of the presence of GF120918.

Similarly, in B-to-A midazolam flux studies, the cumulative amounts of formed 1-OH MDZ at 5 and 10 μM donor midazolam were 59.3 (±5.6) and 73.5 (±9.9) pmol/monolayer without GF120918, and 74.4 (±5.3) and 98.1 (±5.5) pmol/monolayer with GF120918, respectively. Hence, the ratios of cumulative 1-OH MDZ formed with GF120918 vs. without GF120918 were 1.26 (±0.15) and 1.33 (±0.19) for 5 and 10 μM donor midazolam, respectively. Although in qualitative agreement with the above A-to-B results that show a 25% increase in midazolam metabolism due to the presence of GF120918, results here for B-to-A did not show a statistical enhancement in 1-OH MDZ formation because of GF120918 ($p = 0.06$ and 0.06 for 5 and 10 μM).

Although P-gp inhibition resulted in a 25% increase in midazolam metabolism in the A-to-B transport studies, the ER was unchanged, as shown in Fig. 4. At each of the four studied midazolam concentrations, GF120918 did not affect the ER ($p > 0.23$), in agreement with previous findings using apical dosing of 3 μM midazolam with and without GF120918 (10). However, inspection of equation 1 allows for a modest increase in 1-OH MDZ formation with P-gp inhibition with no perceptible change in ER, because ER variability is dependent upon the variability in midazolam flux, in addition to the variability in 1-OH MDZ formation.

Table II lists the ratio of 1-OH MDZ concentrations in the apical and basolateral compartments from each midazolam transport study. Previously, such concentration ratios were found to be about two across a concentration range up to 100 μM (19). This preferential distribution of 1-OH MDZ into the apical compartment was attributed to the proximity of cellular CYP3A to the apical membrane. In Table II, the B-to-A studies yielded similar concentration ratios. For example, from un-induced and induced B-to-A monolayer studies using 5 μM donor midazolam, the concentration ratios were 3.83 and 4.02, respectively. Meanwhile, the A-to-B studies did not indicate any preferential distribution of 1-OH MDZ, but resulted in concentration ratios of about 1.0. An explanation for these observations is not evident. Nevertheless, GF120918 had no effect on the concentration ratio, regardless of midazolam concentration or direction of transport.

DISCUSSION

The above results indicate that P-gp did not markedly affect midazolam's transport, although midazolam stimulates P-gp ATPase and midazolam inhibits P-gp transport of P-gp substrates. Results also indicate P-gp inhibition caused a modest increase in midazolam metabolism at higher midazolam concentrations. One possible explanation is that midazolam is not translocated by P-gp, and inhibits P-gp translocation of other substrates, although it stimulates P-gp ATPase. However, another possible explanation is that midazolam is a P-gp substrate, and can serve to inhibit P-gp efflux of substrates, but that midazolam's high permeability attenuates P-gp's effect on overall midazolam transport kinetics (11). The high permeability of midazolam allows for the possibility that midazolam is a P-gp substrate, whose transport cannot be practically modulated by P-gp due to high midazolam passive membrane permeability. It would generally appear to be difficult to differentiate between these two possibilities.

Results here suggest that midazolam is in fact a P-gp substrate. Midazolam transport was generally not polarized across Caco-2 monolayers or even MDR1-MDCK monolayers. However, across MDR1-MDCK monolayers, GF120918 increased midazolam A-to-B permeability ($p = 0.014$), and intracellular midazolam retention ($p = 0.007$), which perhaps suggest some manifestation of P-gp efflux with midazolam. Further evidence is suggested in the literature. For example, in equilibrium studies across Caco-2 monolayers, midazolam preferentially distributed into the apical compartment by a factor of 1.4 (17,19).

Observations here for midazolam are similar to verapamil, which is highly permeable and interacts with P-gp in a concentration-dependent manner (25). Eytan *et al.* (14,26) suggested that verapamil is a "fast diffuser," i.e., the influx of verapamil across the membrane of P-gp expressing cells would dominate the efflux of verapamil. Perhaps many highly permeable compounds exhibit these properties, including P-gp ATPase activation due to continuous P-gp efflux. For example, in one study, ten of sixty-six compounds, including verapamil and midazolam, activated P-gp ATPase and inhibited calcein AM uptake without manifesting B/A ratio considerably higher than unity (13). A distinguishing feature of this group was their very high permeability.

Table II. Apical vs. Basolateral 1-OH-MDZ Concentration Ratio after Midazolam Transport across Caco-2 Monolayers

Cells	Transport direction	Initial MDZ donor concentration (μM)	Ratio apical/basolateral concentration 1-OH-MDZ without GF120918[a]	Ratio apical/basolateral concentration 1-OH-MDZ with GF120918[a]
Uninduced	A-to-B	5	0.92 (±0.18)	NA[b]
		25	0.92 (±0.30)	NA[b]
		100	0.99 (±0.35)	NA[b]
	B-to-A	5	3.83 (±1.03)	NA[b]
Induced	A-to-B	5	1.35 (±0.17)	1.37 (±0.58)
		10	1.45 (±0.46)	1.21 (±0.25)
		25	0.98 (±0.21)	0.90 (±0.34)
		100	0.96 (±0.17)	1.16 (±0.20)
	B-to-A	5	4.02 (±1.22)	2.10 (±0.62)
		10	3.68 (±1.50)	3.23 (±1.53)

[a] Values in brackets are SEMs of at least triplicate determinations at 40 min.
[b] NA denotes not performed.

The observation here that P-gp inhibition caused a modest increase in 1-OH MDZ formation may also support the hypothesis that midazolam is a P-gp substrate. It has been suggested that P-gp acts in concert with CYP3A4 to limit *in vivo* oral absorption of xenobiotics, such that P-gp action enhances metabolism. Hence, P-gp inhibition of a dual P-gp/CYP3A substrate may be expected to modulate metabolism (e.g. reduce metabolism). Interestingly, in our *in vitro* studies, P-gp inhibition enhanced rather than reduced 1-OH MDZ formation after apical midazolam dosing. This qualitative difference may suggest a fundamental difference in the coupling of P-gp and CYP3A activities *in vitro* and *in vivo*, such as the *in vitro* study being a geometrically simplified approximation of the *in vivo* situation.

In previous *in vitro* transport studies, P-gp inhibition has resulted in increased metabolite production. For example, GF120918 increased the metabolite formation of the dual P-gp /CYP substrate K77; after A-to-B K77 transport, both intracellular and extracellular K77 metabolites increased in the presence of GF120918 (18). Despite increased K77 metabolite formation, the ER for K77 decreased in the presence of GF120918. This reduced ER resulted from significant inhibition of K77 efflux, and hence greater K77 present in the receiver with GF120918 (18).

In part, results here for midazolam parallel results for K77. For midazolam, P-gp inhibition resulted in a modest increase in 1-OH MDZ formation. Unlike K77, midazolam did not exhibit marked polarized transport, which was not markedly changed by GF120918; K77 exhibited polarized transport, which was abolished by GF120918. Underlying this difference in apparent P-gp and CYP3A kinetics is midazolam's 10-fold higher passive membrane permeability. Midazolam's Caco-2 permeability was about 35×10^{-6} cm/s, whereas it appears that K77's passive permeability was approximately 3×10^{-6} cm/s. In addition to passive permeability contributing to apparent P-gp kinetics, passive permeability may contribute to the role of P-gp in modulating metabolism. For midazolam, its high membrane permeability results in the aqueous boundary layer limiting midazolam transport, such that the abolishment of midazolam efflux by GF120918 had essentially no effect on midazolam permeability. However, GF120918 modestly increased midazolam level in the cells, resulting in greater midazolam metabolism. Further investigations would be required to better characterize the role of passive drug permeability in P-gp/metabolism systems. Midazolam may represent a limiting case, where midazolam's high permeability minimizes changes in metabolism due to P-gp inhibition.

Although the present results suggest that midazolam is a P-gp substrate, P-gp exhibits partial substrate overlap with other efflux transporters, such as breast cancer resistance protein (BCRP) and multiresistance associated protein 2 (MRP2). Hence, the present results cannot broadly exclude midazolam to be a substrate for other efflux transporters, or exclude other efflux transporters to contribute to results here, such as GF120918's effect on 1-OH MDZ formation. However, MRP2 is not inhibited by GF120918 (27,28). The potential contribution of BCRP to the results here is less clear. GF120918 is known to inhibit BCRP (29). However, BCRP's low expression in Caco-2 monolayers suggests that BCRP did not contribute toward GF120918s modest enhancement of 1-OH MDZ formation (30).

In summary, the objectives of this study were to assess whether midazolam exhibits characteristics of a highly permeable P-gp substrate and to evaluate the influence of P-gp inhibition on 1-OH MDZ formation during midazolam transport. Results suggest midazolam to be a high permeability P-gp substrate. P-gp inhibition resulted in a slight increase in 1-OH MDZ formation.

REFERENCES

1. M. F. Paine, D. D. Shen, K. L. Kunze, J. D. Perkins, C. L. Marsh, J. P. McVicar, D. M. Barr, B. S. Gillies, and K. E. Thummel. First-pass metabolism of midazolam by the human intestine. *Clin. Pharmacol. Ther.* **60**:14–24 (1996).
2. J. C. Kolars, W. M. Awni, R. M. Merion, and P. B. Watkins. First-pass metabolism of cyclosporin by the gut. *Lancet* **338**:1488–1490 (1991).
3. A. Sparreboom, J. van Asperen, U. Mayer, A. H. Schinkel, J. W. Smit, D. K. Meijer, P. Borst, W. J. Nooijen, J. H. Beijnen, and O. van Tellingen. Limited oral bioavailability and active epithelial excretion of paclitaxel (Taxol) caused by P-glycoprotein in the intestine. *Proc. Natl. Acad. Sci. USA* **94**:2031–2035 (1997).
4. K. S. Lown, R. R. Mayo, A. B. Leichtman, H. L. Hsiao, D. K. Turgeon, P. Schmiedlin-Ren, M. B. Brown, W. Guo, S. J. Rossi, L. Z. Benet, and P. B. Watkins. Role of intestinal P-glycoprotein (mdr1) in interpatient variation in the oral bioavailability of cyclosporine. *Clin. Pharmacol. Ther.* **62**:248–260 (1997).
5. V. J. Wacher, J. A. Silverman, Y. Zhang, and L. Z. Benet. Role of P-glycoprotein and cytochrome P450 3A in limiting oral absorption of peptides and peptidomimetics. *J. Pharm. Sci.* **87**:1322–1330 (1998).
6. V. J. Wacher, C. Y. Wu, and L. Z. Benet. Overlapping substrate specificities and tissue distribution of cytochrome P450 3A and P-glycoprotein: Implications for drug delivery and activity in cancer chemotherapy. *Mol. Carcinog.* **13**:129–134 (1995).
7. L. Z. Benet, T. Izumi, Y. Zhang, J. A. Silverman, and V. J. Wacher. Intestinal MDR transport proteins and P-450 enzymes as barriers to oral drug delivery. *J. Control. Release* **62**:25–31 (1999).
8. S. D. Hall, K. E. Thummel, P. B. Watkins, K. S. Lown, L. Z. Benet, M. F. Paine, R. R. Mayo, D. K. Turgeon, D. G. Bailey, R. J. Fontana, and S. A. Wrighton. Molecular and physical mechanisms of first-pass extraction. *Drug Metab. Dispos.* **27**:161–166 (1999).
9. L. Y. Li, G. L. Amidon, J. S. Kim, T. Heimbach, F. Kesisoglou, J. T. Topliss, and D. Fleisher. Intestinal metabolism promotes regional differences in apical uptake of indinavir: Coupled effect of P-glycoprotein and cytochrome P450 3A on indinavir membrane permeability in rat. *J. Pharmacol. Exp. Ther.* **301**:586–593 (2002).
10. L. Z. Benet and C. L. Cummins. The drug efflux-metabolism alliance: biochemical aspects. *Adv. Drug Deliv. Rev.* **50**(Suppl 1):S3–11 (2001).
11. K. A. Lentz, J. W. Polli, S. A. Wring, J. E. Humphreys, and J. E. Polli. Influence of passive permeability on apparent P-glycoprotein kinetics. *Pharm. Res.* **17**:1456–1460 (2000).
12. S. Doppenschmitt, H. Spahn-Langguth, C. G. Regardh, and P. Langguth. Role of P-glycoprotein-mediated secretion in absorptive drug permeability: An approach using passive membrane permeability and affinity to P-glycoprotein. *J. Pharm. Sci.* **88**:1067–1072 (1999).
13. J. W. Polli, S. A. Wring, J. E. Humphreys, L. Huang, J. B. Morgan, L. O. Webster, and C. S. Serabjit-Singh. Rational use of in vitro P-glycoprotein assays in drug discovery. *J. Pharmacol. Exp. Ther.* **299**:620–628 (2001).
14. G. D. Eytan, R. Regev, G. Oren, and Y. G. Assaraf. The role of passive transbilayer drug movement in multidrug resistance and its modulation. *J. Biol. Chem.* **271**:12897–12902 (1996).
15. R. N. Upton, G. L. Ludbrook, C. Grant, and A. Martinez. In vivo cerebral pharmacokinetics and pharmacodynamics of diazepam and midazolam after short intravenous infusion administration in sheep. *J. Pharmacokinet. Pharmacodyn.* **28**:129–153 (2001).

16. R. Amrein and W. Hetzel. Pharmacology of Dormicum (midazolam) and Anexate (flumazenil). *Acta Anaesthesiol. Scand. Suppl.* **92**:6–15 (1990).
17. P. Schmiedlin-Ren, K. E. Thummel, J. M. Fisher, M. F. Paine, K. S. Lown, and P. B. Watkins. Expression of enzymatically active CYP3A4 by Caco-2 cells grown on extracellular matrix-coated permeable supports in the presence of 1alpha,25-dihydroxyvitamin D3. *Mol. Pharmacol.* **51**:741–754 (1997).
18. C. L. Cummins, W. Jacobsen, and L. Z. Benet. Unmasking the dynamic interplay between intestinal P-glycoprotein and CYP3A4. *J. Pharmacol. Exp. Ther.* **300**:1036–1045 (2002).
19. J. M. Fisher, S. A. Wrighton, P. B. Watkins, P. Schmiedlin-Ren, J. C. Calamia, D. D. Shen, K. L. Kunze, and K. E. Thummel. First-pass midazolam metabolism catalyzed by 1alpha,25-dihydroxy vitamin D3-modified Caco-2 cell monolayers. *J. Pharmacol. Exp. Ther.* **289**:1134–1142 (1999).
20. R. L. Shepard, M. A. Winter, S. C. Hsaio, H. L. Pearce, W. T. Beck, and A. H. Dantzig. Effect of modulators on the ATPase activity and vanadate nucleotide trapping of human P-glycoprotein. *Biochem. Pharmacol.* **56**:719–727 (1998).
21. J. E. Polli, G. S. Rekhi, L. L. Augsburger, and V. P. Shah. Methods to compare dissolution profiles and a rationale for wide dissolution specifications for metoprolol tartrate tablets. *J. Pharm. Sci.* **86**:690–700 (1997).
22. S. Tolle-Sander and J. E. Polli. Method Considerations for Caco-2 Permeability Assessment in the Biopharmaceutics Classification System. *Pharmacopeial Forum* **28**:164–172 (2002).
23. P. Schmiedlin-Ren, K. E. Thummel, J. M. Fisher, M. F. Paine, and P. B. Watkins. Induction of CYP3A4 by 1 alpha,25-dihydroxyvitamin D3 is human cell line-specific and is unlikely to involve pregnane X receptor. *Drug Metab. Dispos.* **29**:1446–1453 (2001).
24. R. M. Arendt, D. J. Greenblatt, R. H. deJong, J. D. Bonin, D. R. Abernethy, B. L. Ehrenberg, H. G. Giles, E. M. Sellers, and R. I. Shader. In vitro correlates of benzodiazepine cerebrospinal fluid uptake, pharmacodynamic action and peripheral distribution. *J. Pharmacol. Exp. Ther.* **227**:98–106 (1983).
25. T. Litman, T. E. Druley, W. D. Stein, and S. E. Bates. From MDR to MXR: new understanding of multidrug resistance systems, their properties and clinical significance. *Cell. Mol. Life Sci.* **58**: 931–959 (2001).
26. G. D. Eytan, R. Regev, G. Oren, C. D. Hurwitz, and Y. G. Assaraf. Efficiency of P-glycoprotein-mediated exclusion of rhodamine dyes from multidrug-resistant cells is determined by their passive transmembrane movement rate. *Eur. J. Biochem.* **248**: 104–112 (1997).
27. R. Evers, M. Kool, A. J. Smith, L. van Deemter, M. de Haas, and P. Borst. Inhibitory effect of the reversal agents V-104, GF120918 and Pluronic L61 on MDR1 Pgp-, MRP1- and MRP2-mediated transport. *Br. J. Cancer* **83**:366–374 (2000).
28. A. Wallstab, M. Koester, M. Bohme, and D. Keppler. Selective inhibition of MDR1 P-glycoprotein-mediated transport by the acridone carboxamide derivative GG918. *Br. J. Cancer* **79**:1053–1060 (1999).
29. M. Maliepaard, M. A. van Gastelen, A. Tohgo, F. H. Hausheer, R. C. van Waardenburg, L. A. de Jong, D. Pluim, J. H. Beijnen, and J. H. Schellens. Circumvention of breast cancer resistance protein (BCRP)-mediated resistance to camptothecins in vitro using non-substrate drugs or the BCRP inhibitor GF120918. *Clin. Cancer Res.* **7**:935–941 (2001).
30. J. Taipalensuu, H. Tornblom, G. Lindberg, C. Einarsson, F. Sjoqvist, H. Melhus, P. Garberg, B. Sjostrom, B. Lundgren, and P. Artursson. Correlation of gene expression of ten drug efflux proteins of the ATP-binding cassette transporter family in normal human jejunum and in human intestinal epithelial Caco-2 cell monolayers. *J. Pharmacol. Exp. Ther.* **299**:164–170 (2001).